



# Numerical SPIS-Dust Modelling of Plasma – Lunar Lander Interactions

Gennady G. Dolnikov<sup>(1)</sup>, Ilia A. Kuznetsov<sup>(1)</sup>, Alexander V. Zakharov<sup>(1)</sup>, Elena Seran<sup>(2)</sup>,  
Sebastian L.G. Hess<sup>(3)</sup>, Fabrice Cipriani<sup>(4)</sup>, Andrew N. Lyash<sup>(1)</sup>, Inna A. Shashkova<sup>(1)</sup>

<sup>1</sup> *Space Research Institute of Russian Academy of Sciences, Moscow, Russian Federation;*

<sup>2</sup> *LATMOS, Paris, France*

<sup>3</sup> *French Aerosp. Lab., ONERA, Toulouse, France;*

<sup>4</sup> *ESTEC/TEC-EES, Noordwijk, The Netherlands*

*kia@iki.rssi.ru*

# Motivation

- **Global**

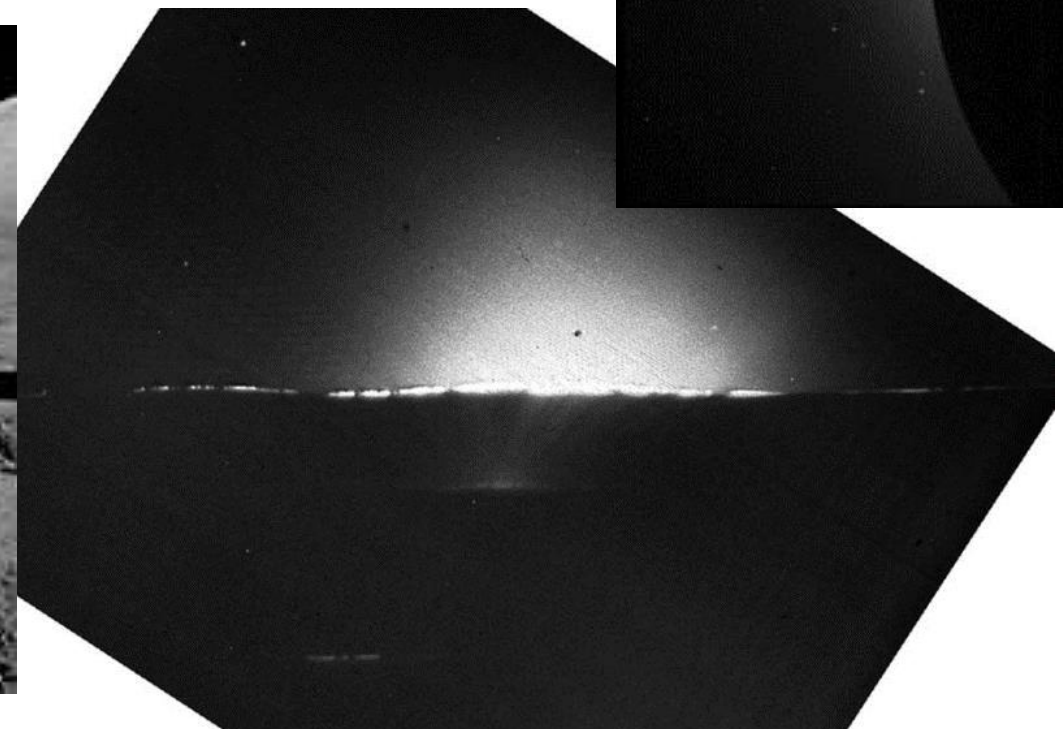
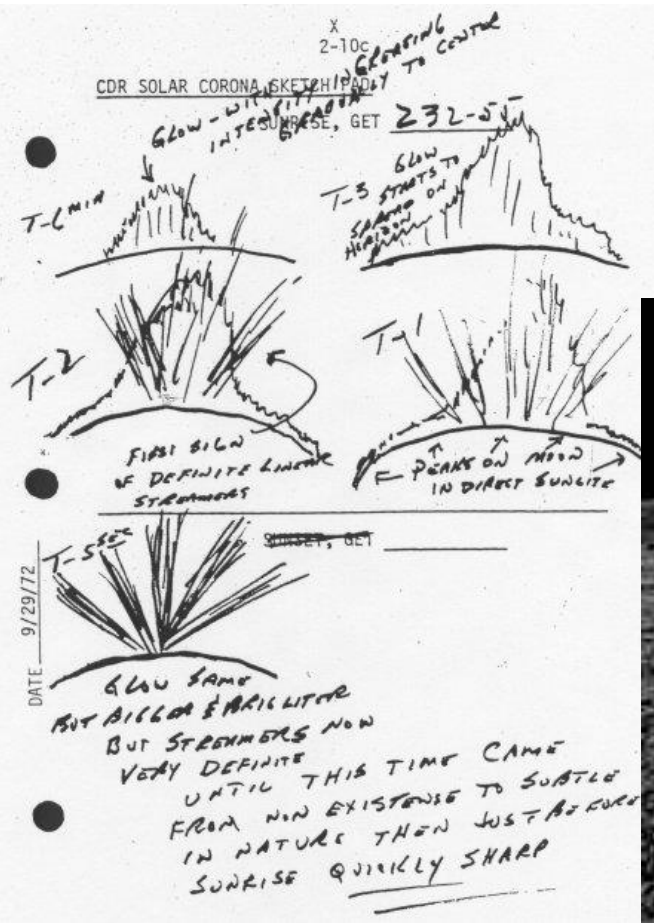
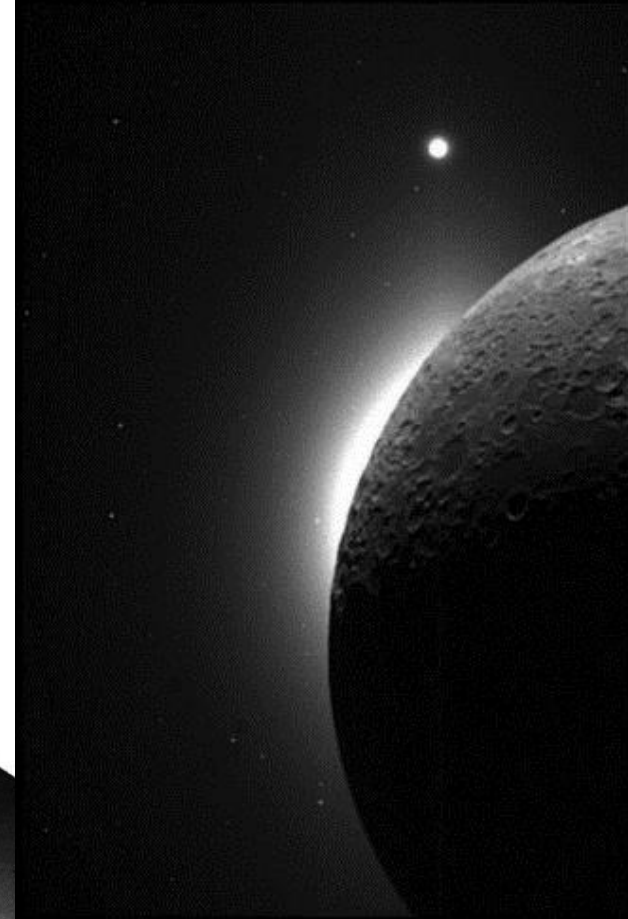
- Understanding the lunar dusty plasma environment, including investigation of the dust electrostatic transport
- Investigation of the spacecraft–exosphere interactions near the surface of the Moon (Phobos, Mercury, other atmosphereless bodies)
- Dusty hazard problem

- **In case of lunar dust and plasma instruments**

- Investigation of the Langmuir probes interaction with lunar dusty plasma environment, effect estimation
- Dust fluxes estimation for Impact sensors

All celestial bodies without the atmosphere are covered with a thin layer of dust. These dust particles are a threat for exploration spacecrafts and instruments and sure for the astronauts.

Dust particles can adhere to lander surfaces. Their irregular shape may cause damages of the lander elements.



# Luna-25 (Luna-Glob) Spacecraft

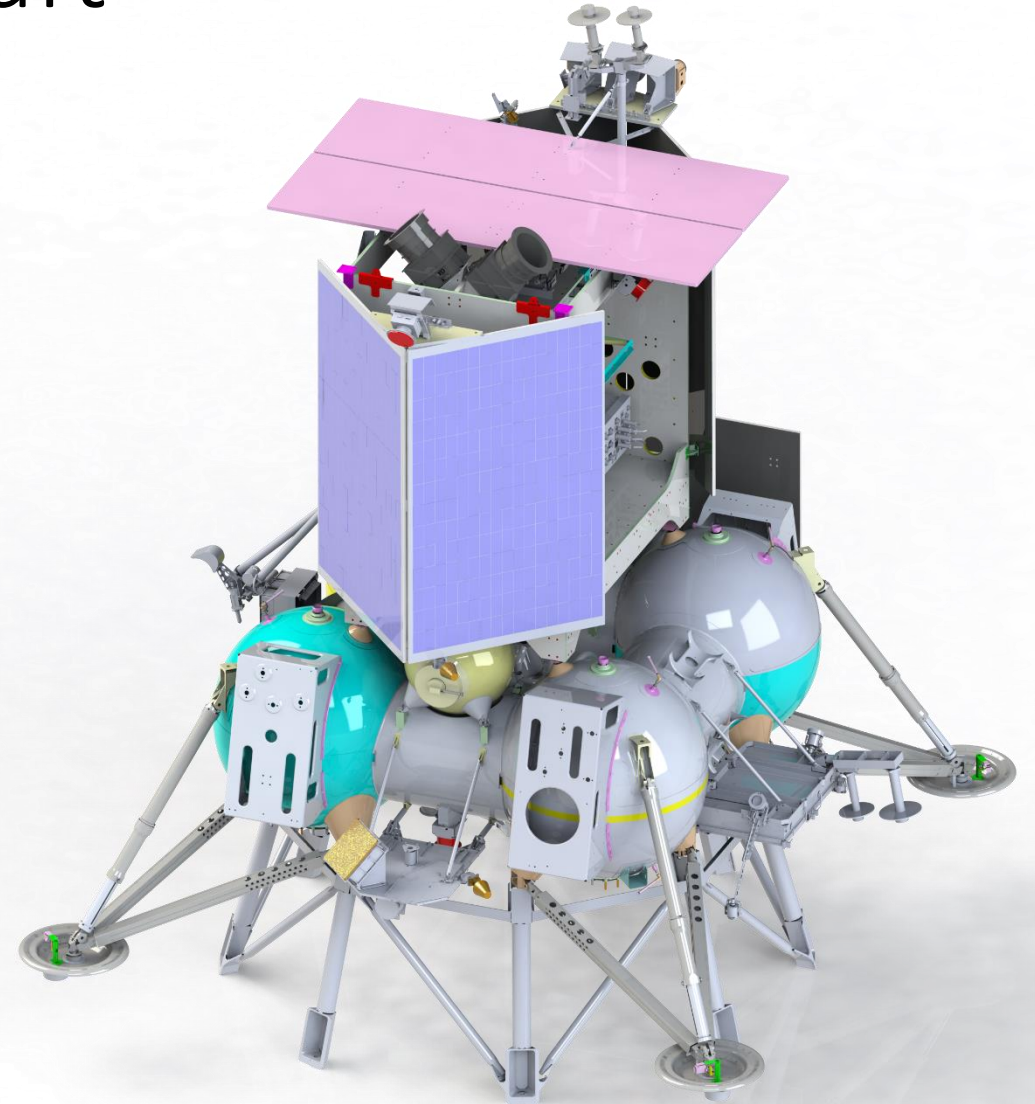
- Luna-25 may be launched ~~in late 2019~~ (actually no)
- The landing side of the Luna-Glob mission is still the matter of discussion, however supposed landing site is bound by  $65^{\circ} \div 85^{\circ}$  S and  $0^{\circ} \div 60^{\circ}$  E, near the South Pole.

Location	Latitude	Longitude
South 1	$76,8^{\circ}$ S	$26,5^{\circ}$ E
South 2	$73,3^{\circ}$ S	$43,9^{\circ}$ E
South 3	$72,9^{\circ}$ S	$41,3^{\circ}$ E

(Kazmerchuk et al., 2016)

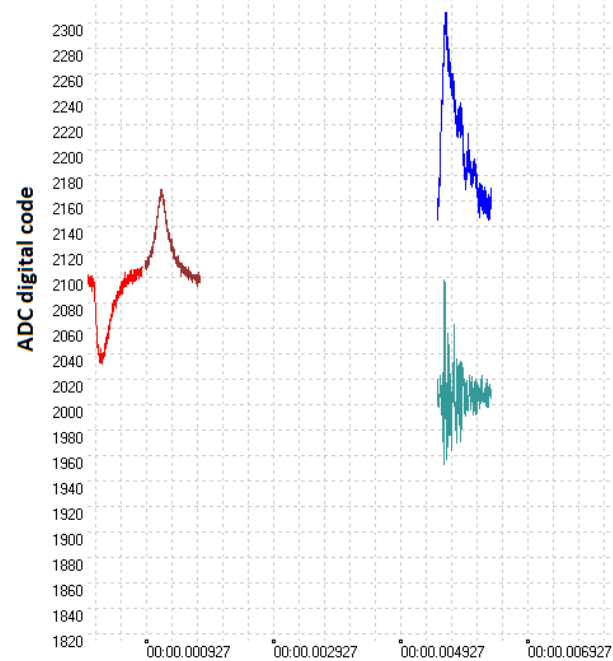
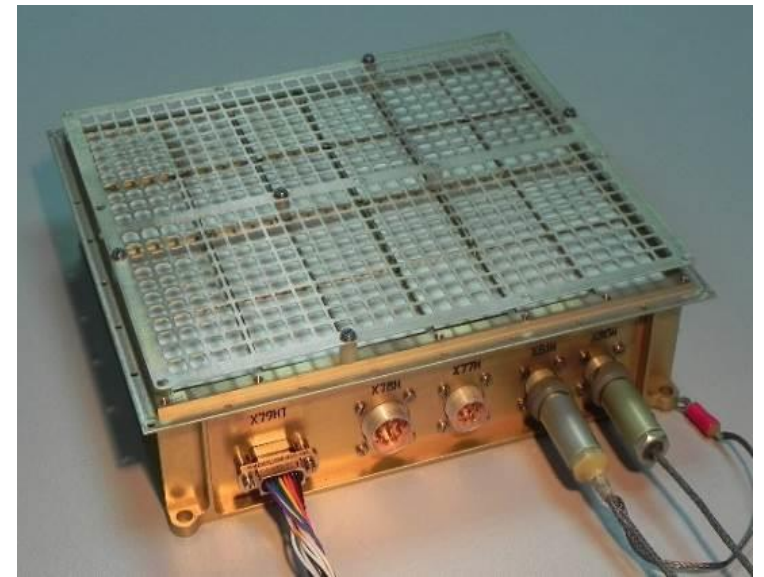
Location	Latitude	Longitude
South 1	$68,8^{\circ}$ S	$21,2^{\circ}$ E
South 2	$68,6^{\circ}$ S	$11,6^{\circ}$ E
South 3	$69,5^{\circ}$ S	$43,5^{\circ}$ E

(Djachkova et al., 2017)

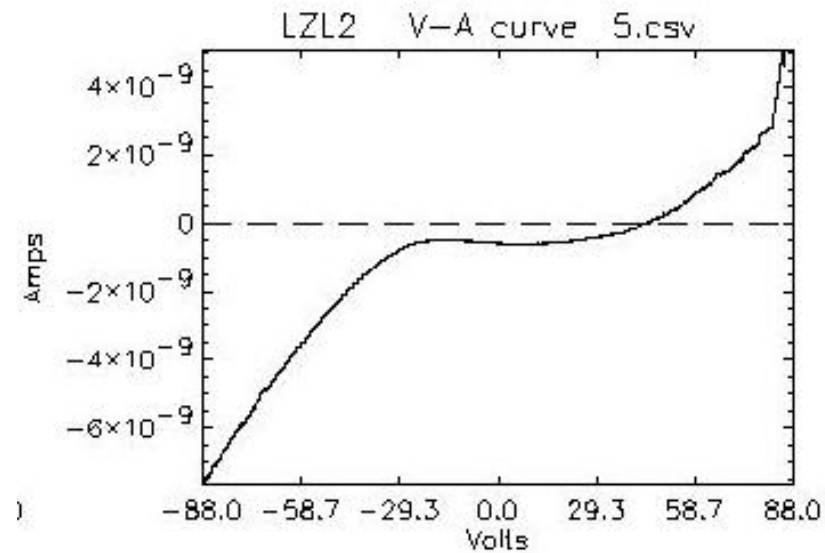


# PmL Dust Instrument

The payload of the Luna-Glob spacecraft includes an instrument PmL for study of dust particles dynamics over the lunar surface and sensors for estimation of the electric field under the surface. The PmL device comprises three units: the Impact Sensor (IS) and 2 electrostatic probes (EP).



Experiment duration, s  
Impact of the dust particle  
( $2 \cdot 10^{-10}$  N·s) in vacuum set-up

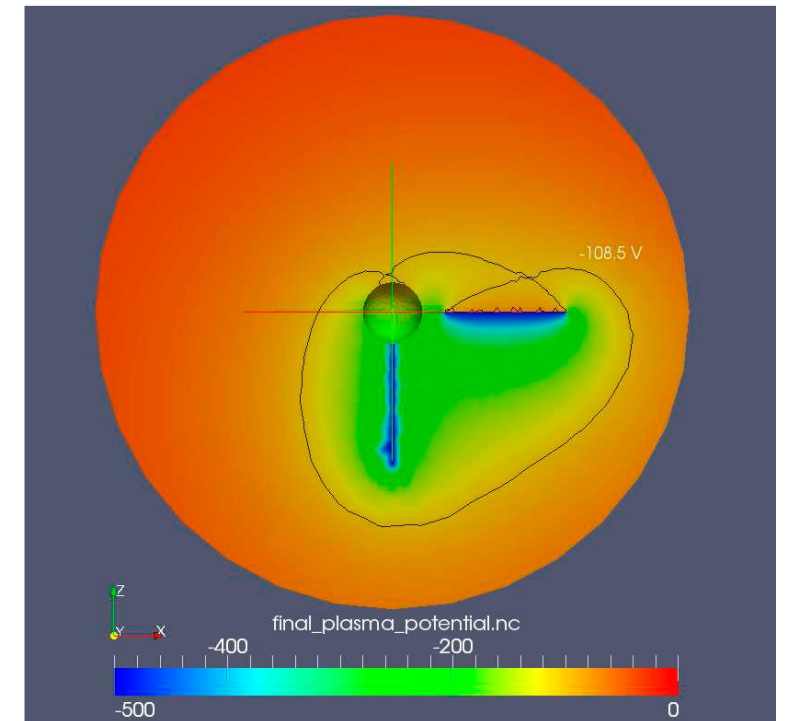


Example of current-voltage curve of  
Langmuir probe from electron populated  
vacuum chamber  
(Thermal emission W e-source with 9V  
0.92A current)

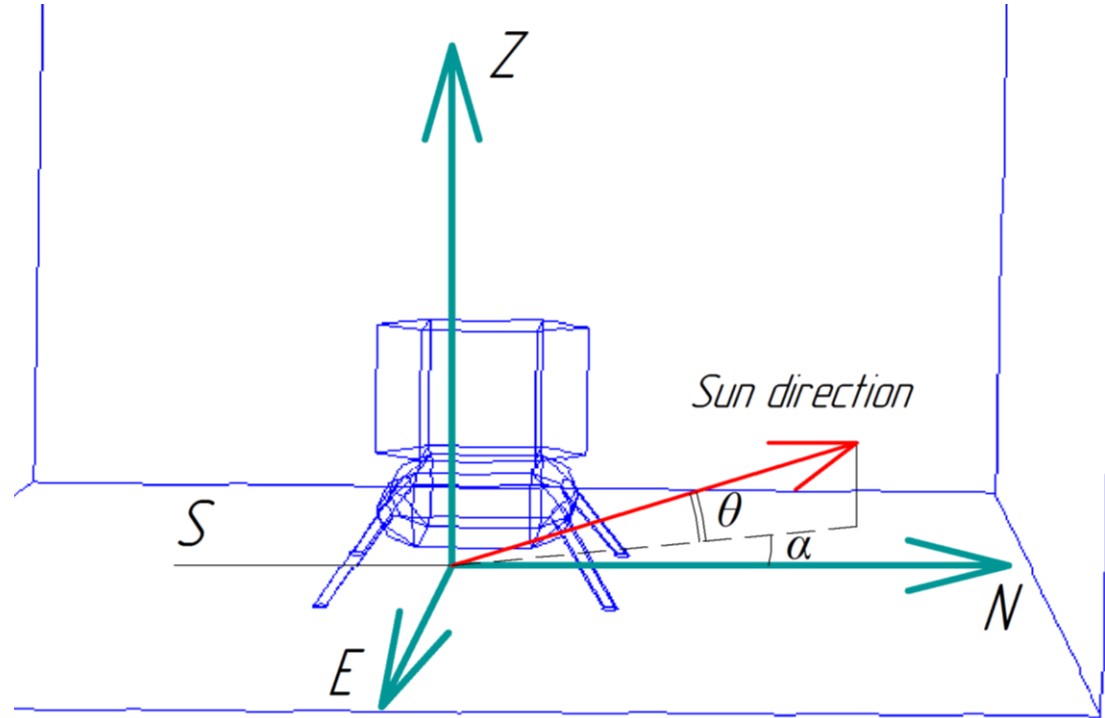
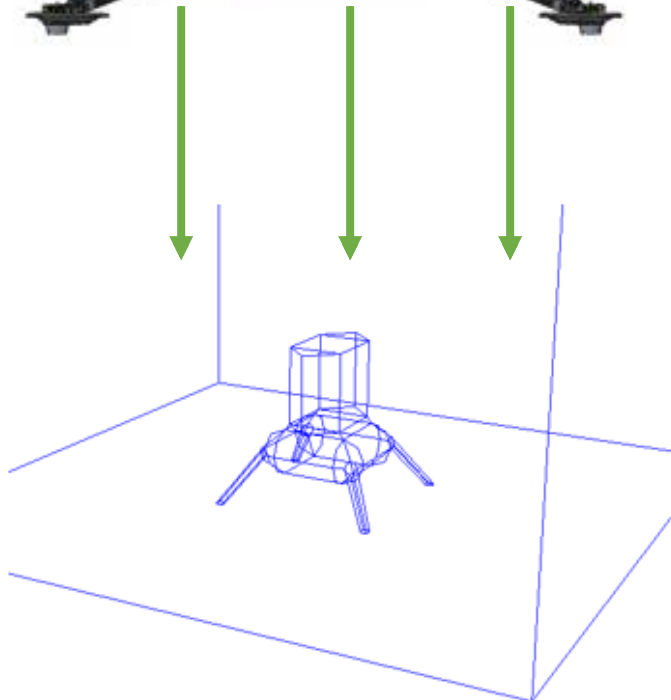
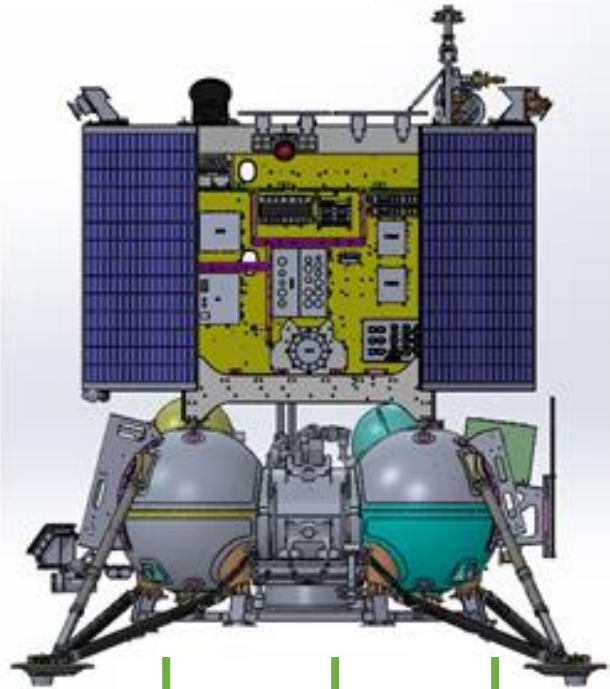


# Why SPIS?

- Simulates the plasma around spacecraft and the spacecraft surface charging. The version 5.1 SPIS includes the “Science” package allowing to simulate the observation of various scientific instruments [S. Hess]
- Dusts are characterized by:
  - - radius
  - - mass depending on the radius
  - - charge that may vary
- All these characteristics are different for each particle. They are defined as distributions.
- Dust feels extra forces:
  - - gravity
  - - photon pressure
- Dusts have some particular interaction:
  - - charge collection (computed through OML or MCC)
  - - SEEE, model of Chow et al., 1999 is implemented
  - - photo-emission (Feuerbacher 1973)
- These interactions lead to the evolution of their charge.



# Spacecraft modelling



10x10x60 m simulation box

Situation	$\alpha$	$\theta$
Local Noon	0°	22°
Local Evening	45°	11°
Sunset	90°	1°

# Conditions

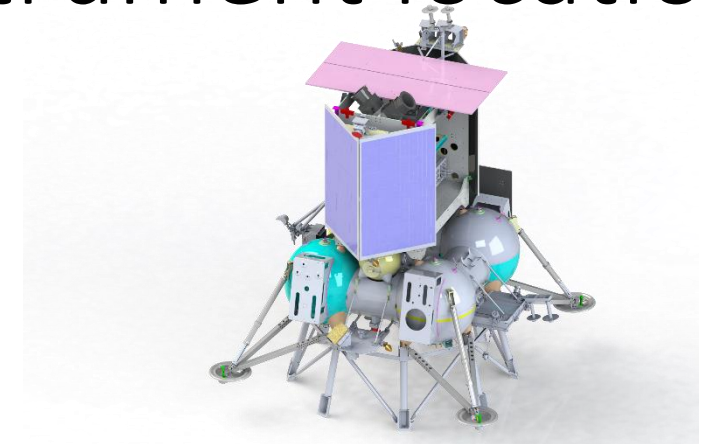
PLASMA CONDITIONS		
PARAMETER	UNIT	VALUE
Ion density, $n_i$	$\text{cm}^{-3}$	10
Electron density, $n_e$	$\text{cm}^{-3}$	10
Ion speed, $V_i$	$\text{km}\cdot\text{s}^{-1}$	430
Electron speed, $V_e$	$\text{km}\cdot\text{s}^{-1}$	430
Ion temperature, $T_i$	eV	10
Electron temperature, $T_e$	eV	10
Photoelectron temperature, $T_{\text{ph}}$	eV	2

[MRAD “Modelling requirements”, 2013; Feuerbacher et al., 1972]

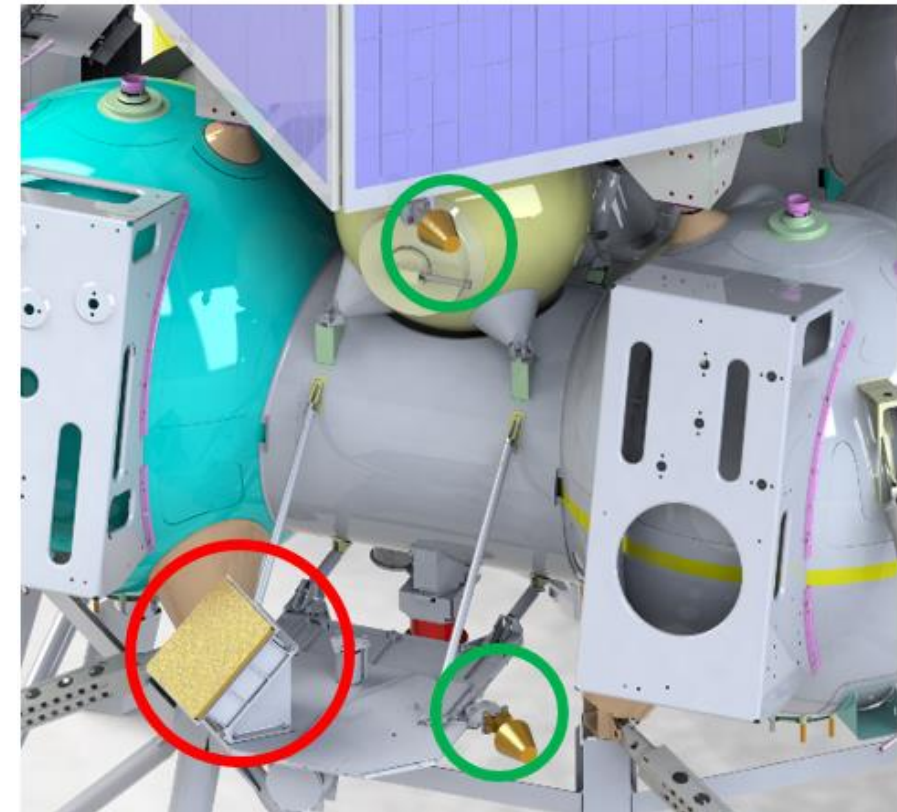


# Surface and material conditions, instrument locations

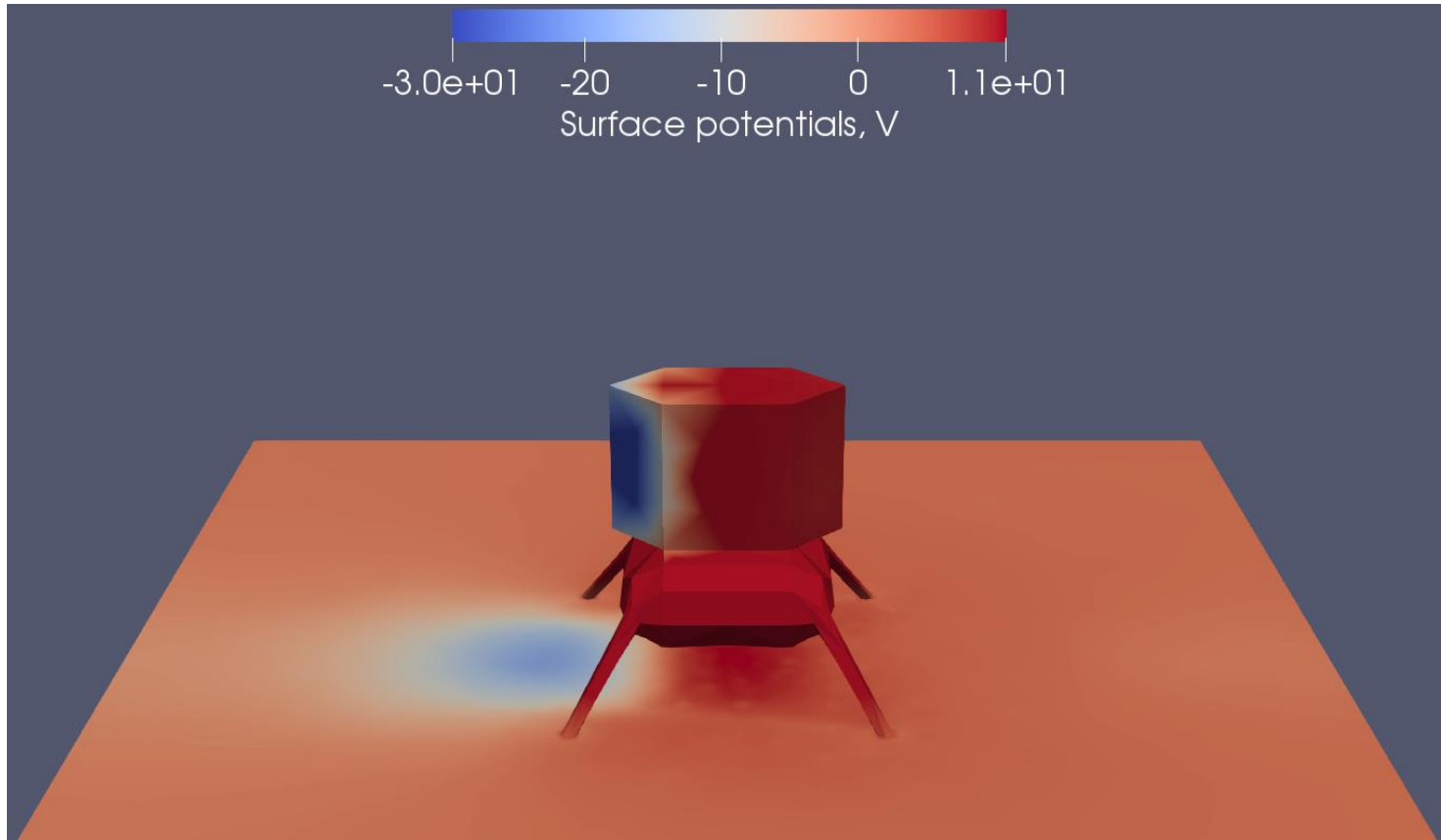
Situation	Lunar Surface Potential, V	North solar panel potential, V	Lunar Surface Temperature, K
Local Noon	0	0	288
Local Evening	0	27	240
Sunset	-10	5	130



- RITs and RITEGs onboard ->  $\sim 233$  K on the “cold” state after the thermal modelling
- density of lunar dust layer of  $1500 \text{ kg/m}^3$  [D.A. Kring, 2006]
- the mass density of dust particles is taken as  $3000 \text{ kg/m}^3$
- the default dust size distribution from 71501,1 Mare sample
- the lander has one equipotential surface made of oxidized aluminum and gold layer of thermal shielding except the SA
- SA made of cerium doped silicon glass and have an initial potentials: 0 V for the south and  $\sim 27$  V north
- no magnetospheric tale
- no magnetic anomalies



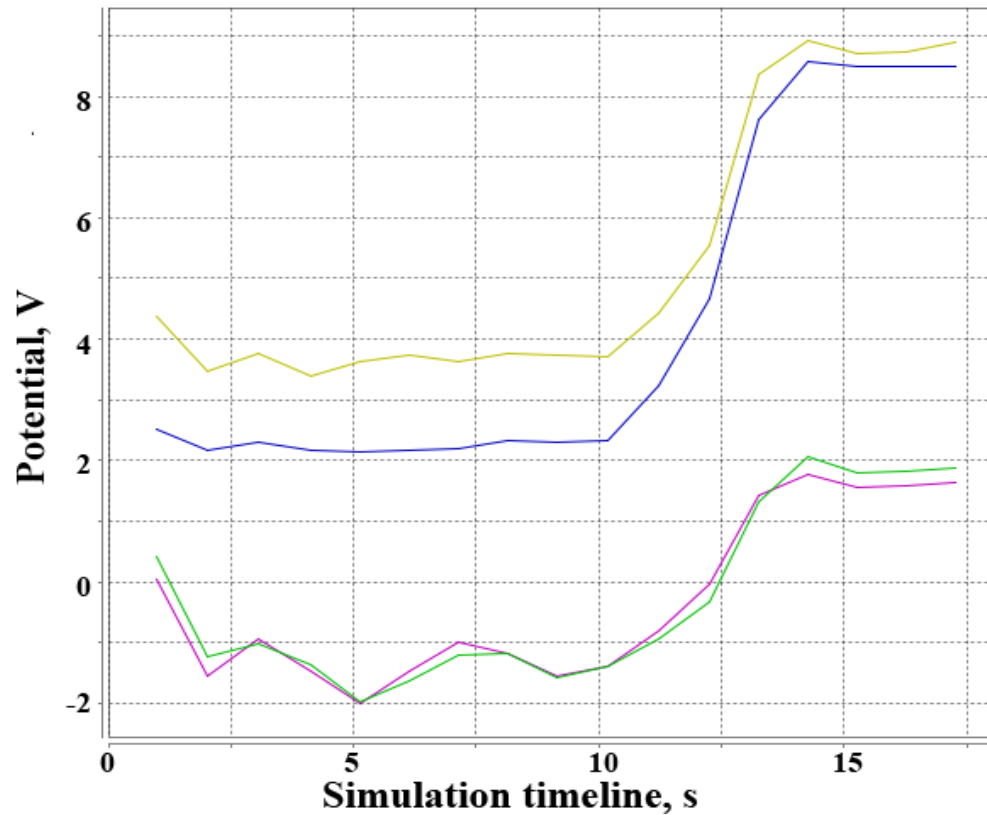
# Results: Surface potentials, Noon conditions



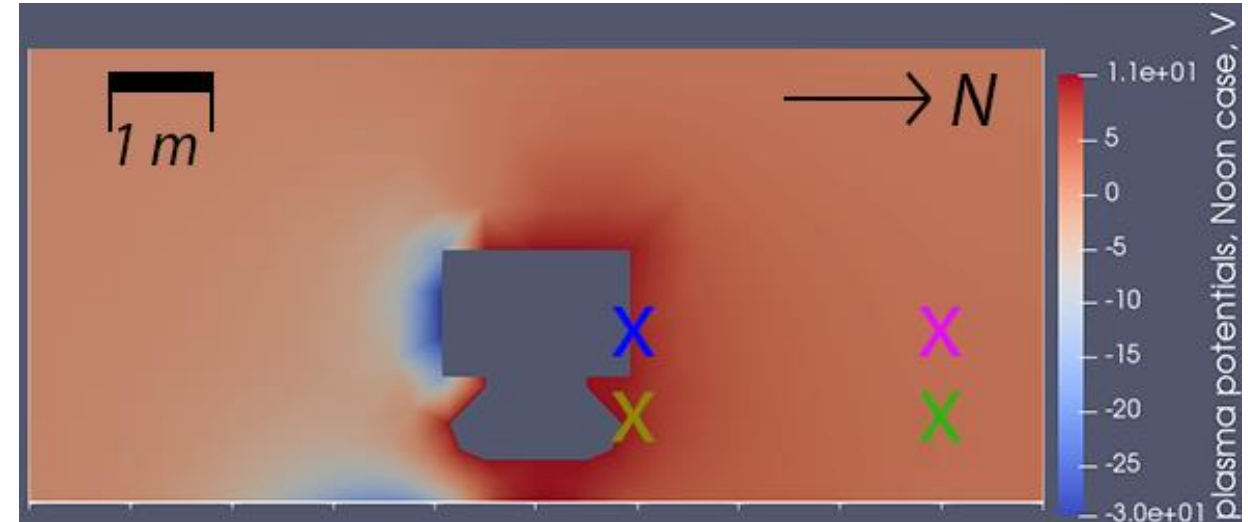
For Luna-Glob we can estimate the positive charging of the conductive (and grounded) SC surfaces mainly due to photoelectron emission processes, the stronger positive charge of the sunlit dielectric surface (north solar panel in our case) and negative charge of dielectric surface in shadow (south solar panel) due to solar wind and plasma electrons collection. Thus, surface charges are the reason of the relatively positive (e.g. around the sunlit solar panel) or negative (e.g. around the shadowed solar panel) sheath around the spacecraft. We also can see them on Plasma Potentials Figures.

Lunar and SC surface potentials after the “Noon” conditions simulation.

# Results: Plasma potentials, Noon conditions

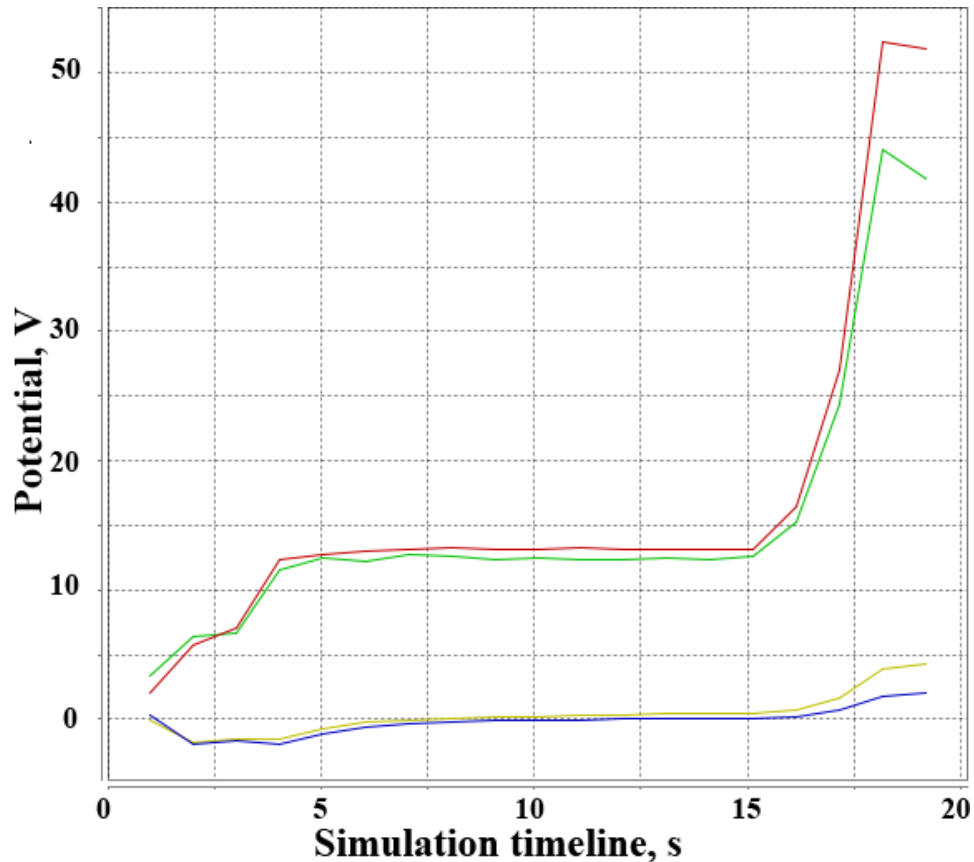


Plasma potentials for the “Noon” simulation: lower (1 m above the surface) and higher (2 m) potentials in the SC vicinity (yellow and blue lines respectively), which correspond with EP sensors positions; the potentials on the 3 m distance from the SC body on the same levels respectively (green and purple) which represent the plasma potentials in undisturbed exosphere.

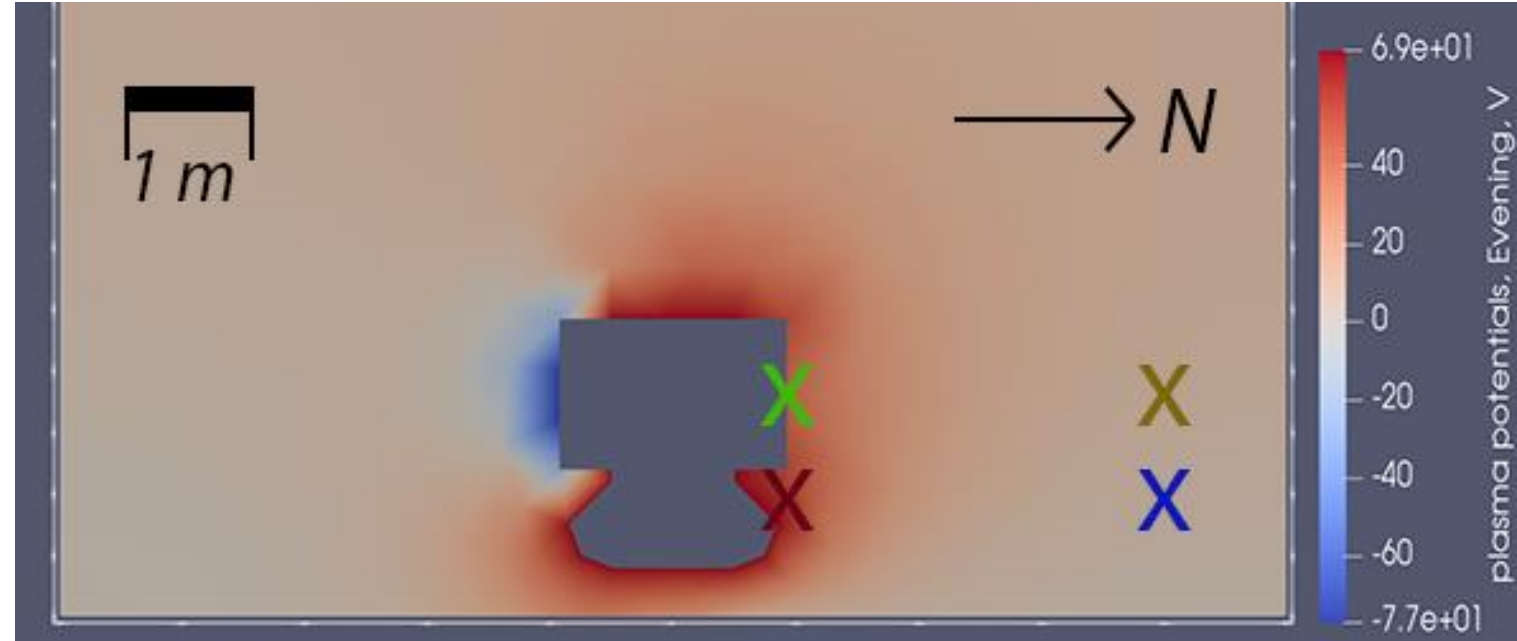


Plasma potentials at the steady-state in the “Noon” conditions. Sun is on the right. Virtual plasma potential sensors in SPIS simulation marked by “X” signs. Two of them matches with locations of the EP sensors on SC. We can see the strong positive bias in the SC vicinity in relation to undisturbed exosphere plasma. However, we have the strongly negative bias in the south (shadow) solar panel vicinity

# First results: Plasma potentials, evening

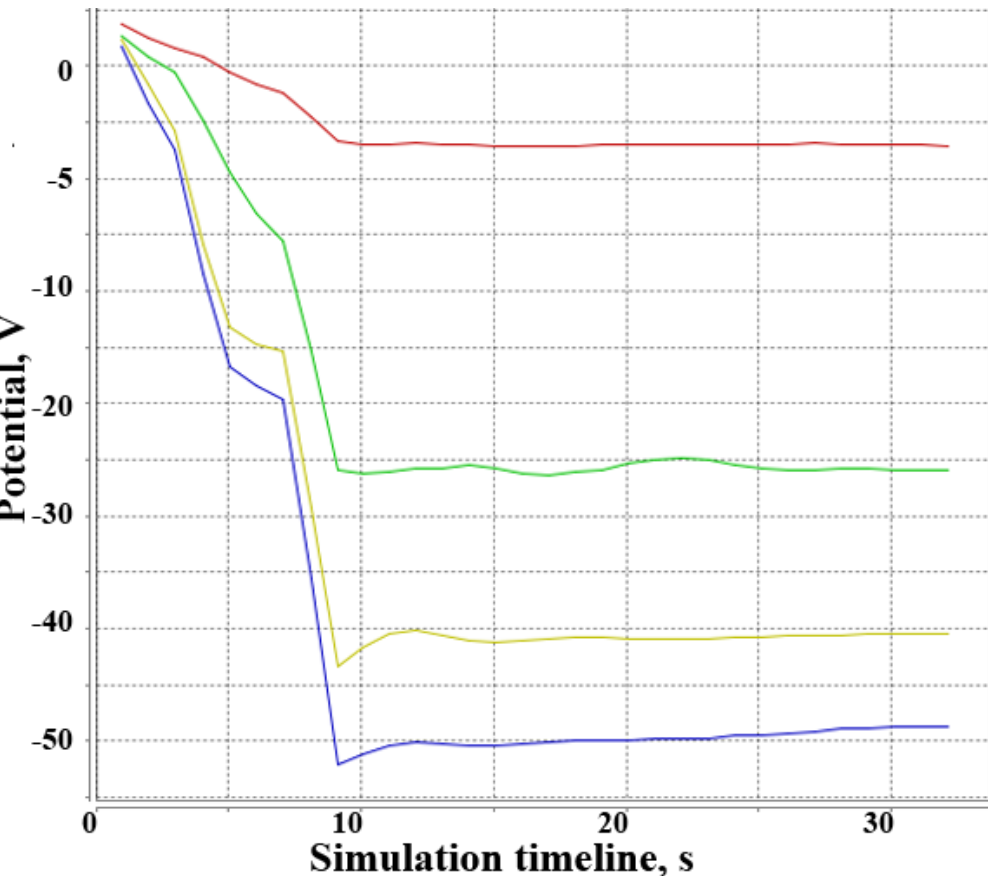


Plasma potentials for the “Evening” simulation: lower (1 m above the surface) and higher (2 m) potentials in the SC vicinity (green and red lines respectively), which correspond with EP sensors positions; the potentials on the 3 m distance from the SC body on the same levels respectively (blue and yellow) which represent the plasma potentials in undisturbed exosphere.

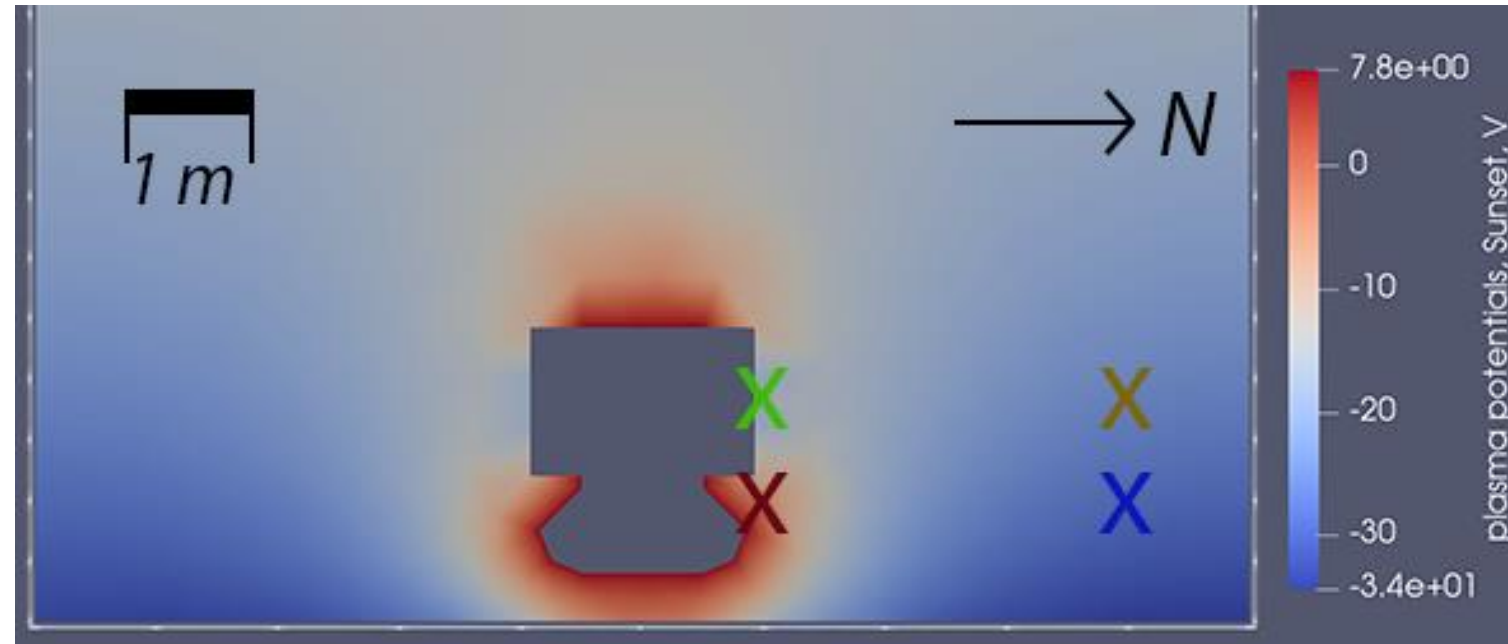


Plasma potentials at the steady state of simulation in “Evening” conditions. Sun is on the right. Virtual plasma potential sensors in SPIS simulation marked by “X” signs. Two of them matches with locations of the EP sensors on SC. We can see the stronger positive bias in SC vicinity in relation to undisturbed exosphere plasma.

# First results: Plasma potentials, sunset

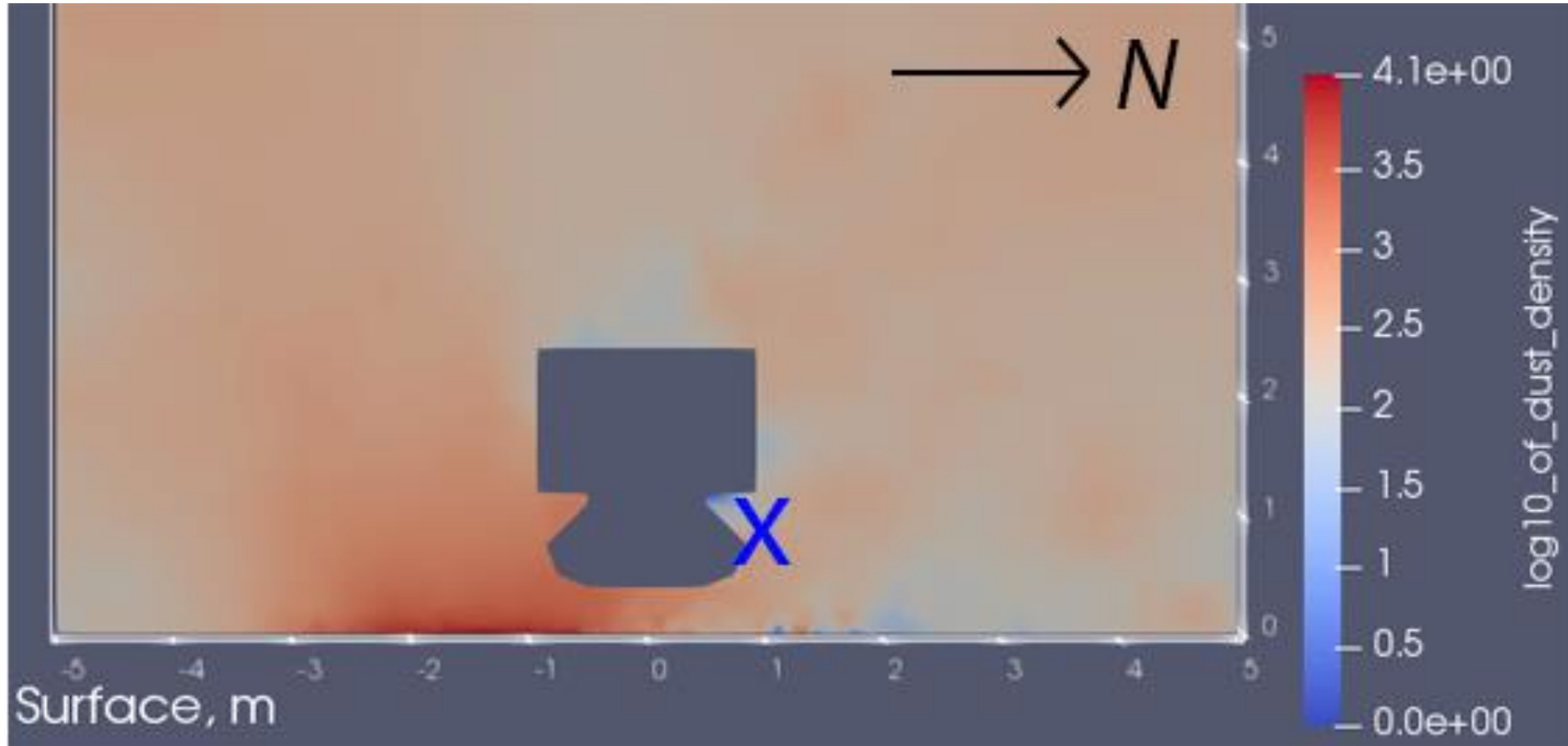


Plasma potentials for the “Sunset” simulation: lower (1 m above the surface) and higher (2 m) potentials in the SC vicinity (green and red lines respectively), which correspond with EP sensors positions; the potentials on the 3 m distance from the SC body on the same levels respectively (blue and yellow) which represent the plasma potentials in undisturbed exosphere.

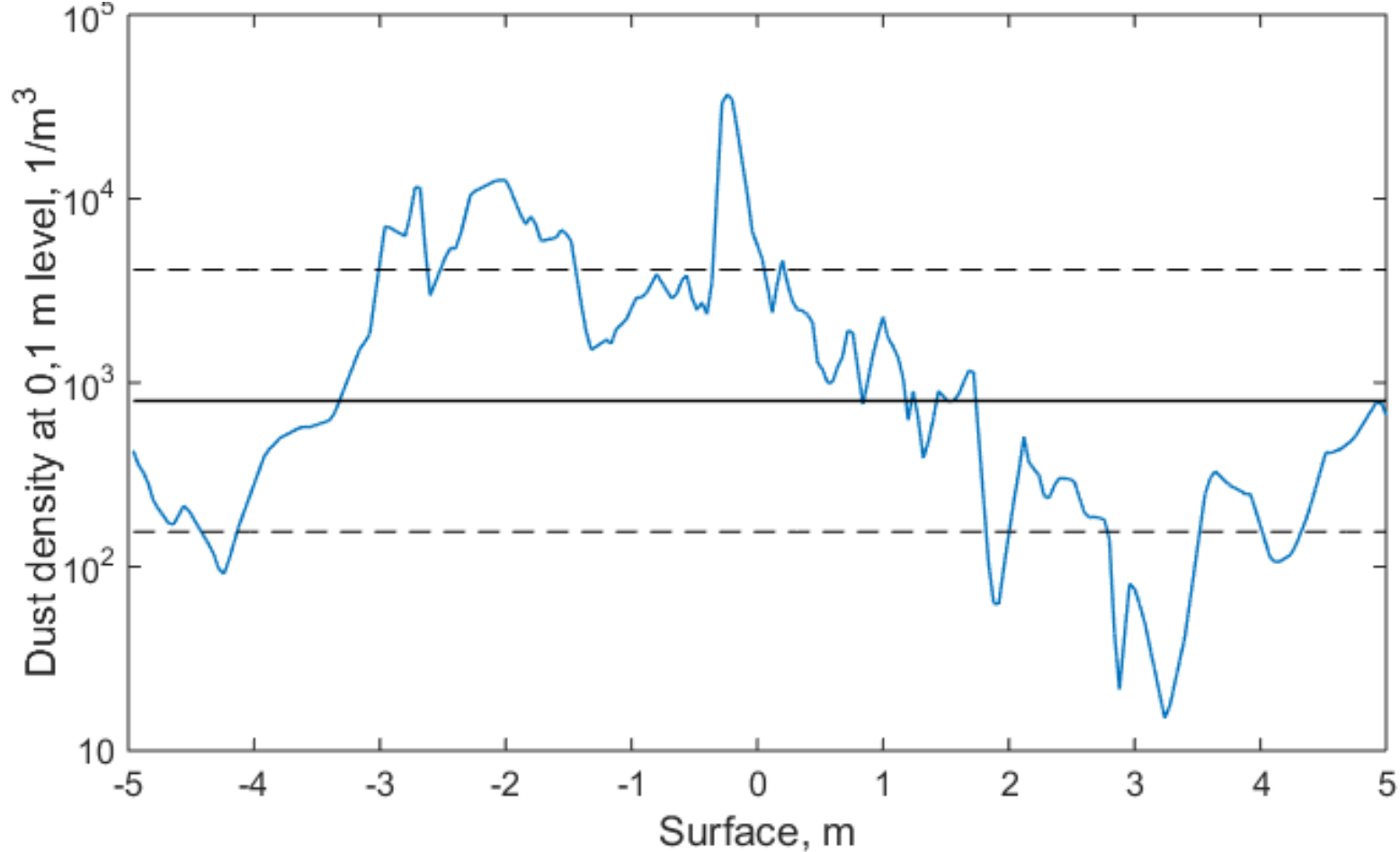


Plasma potentials at the steady state of simulation in “Sunset” conditions. Sun is behind the SC, 1° above the horizon. Virtual plasma potential sensors in SPIS simulation marked by “X” signs. Two of them (red, green) matches with locations of the EP sensors on SC.

# Dust densities

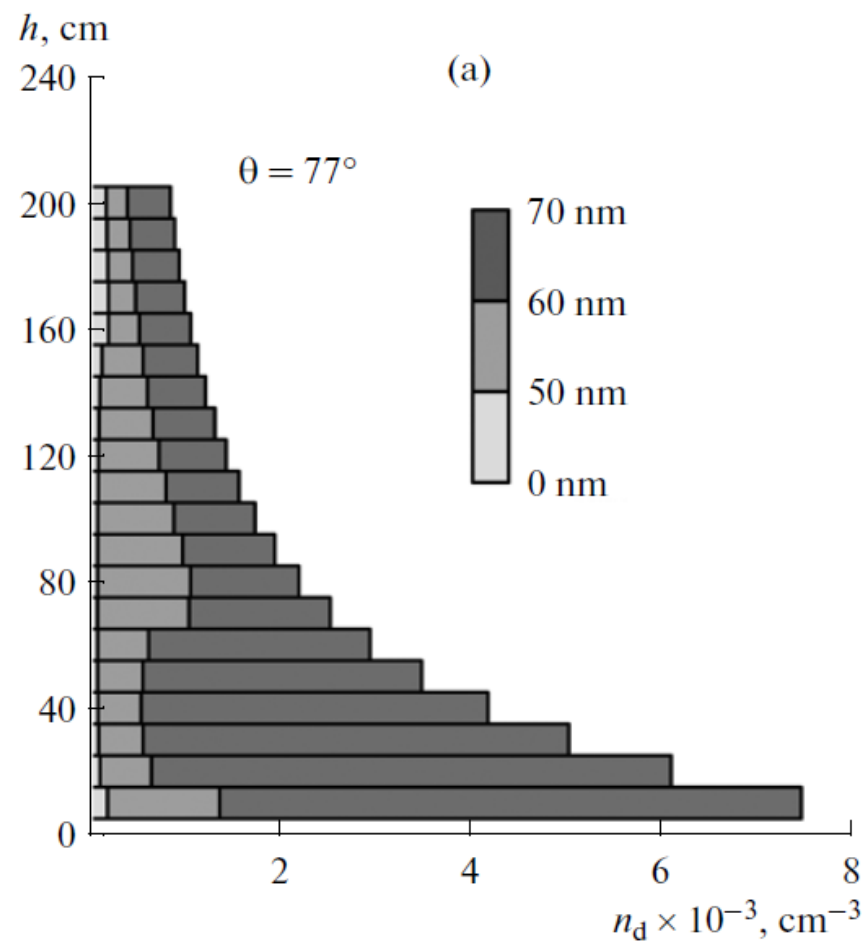


Common logarithm of the dust density in particles per cubic meter at the local lunar noon. The sun is on the right, 22° above the horizon. IS from the PmL instrument location marked by "X" sign.

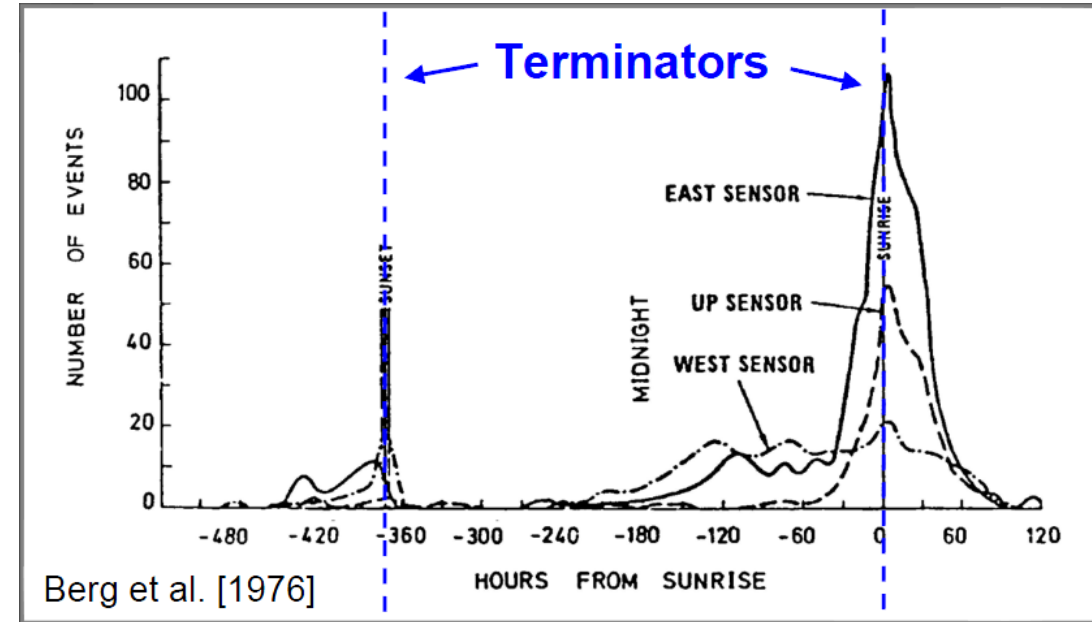


Dust density at 0,1 m level at the “Local Noon” simulation results (blue) and it’s average  $7.9 \cdot 10^2 \text{ m}^{-3}$  (black line) with error of  $\pm 6 \cdot 10^2 \text{ m}^{-3}$  (dashed line).

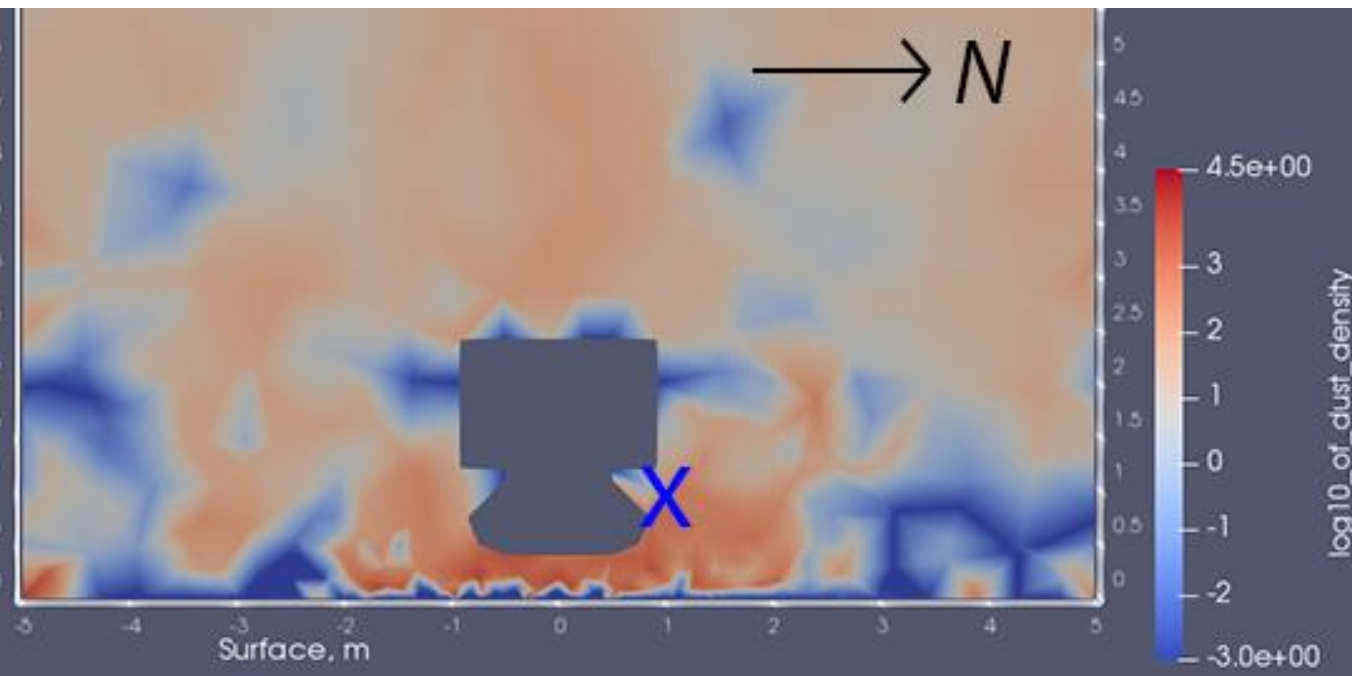
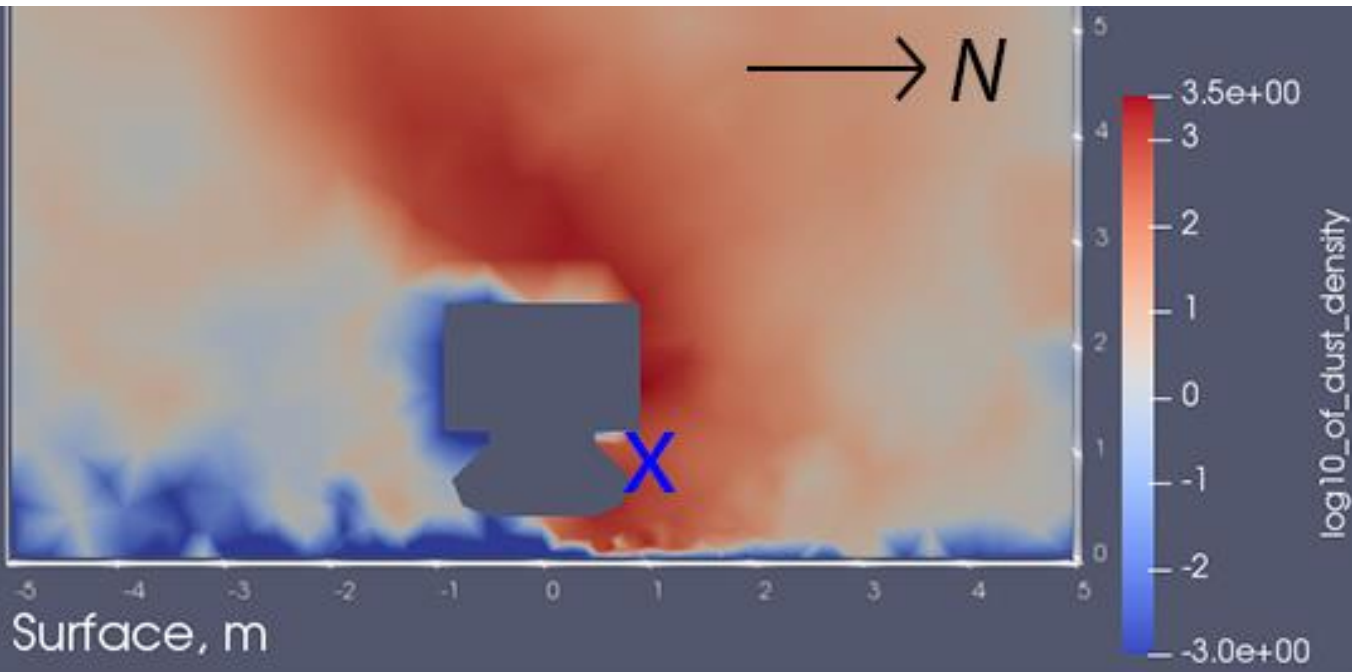
These results correspond to the theoretical model (Popel et al., 2013), where values of dust density vary from  $4.5 \cdot 10^3 \text{ m}^{-3}$  to  $7.5 \cdot 10^{10} \text{ m}^{-3}$  near the lunar surface (from 0 to 10 cm) depending on latitude (from  $77^\circ$  to  $87^\circ$ ).



# Apollo 17 Lunar Ejecta and Meteorites (LEAM) experiment



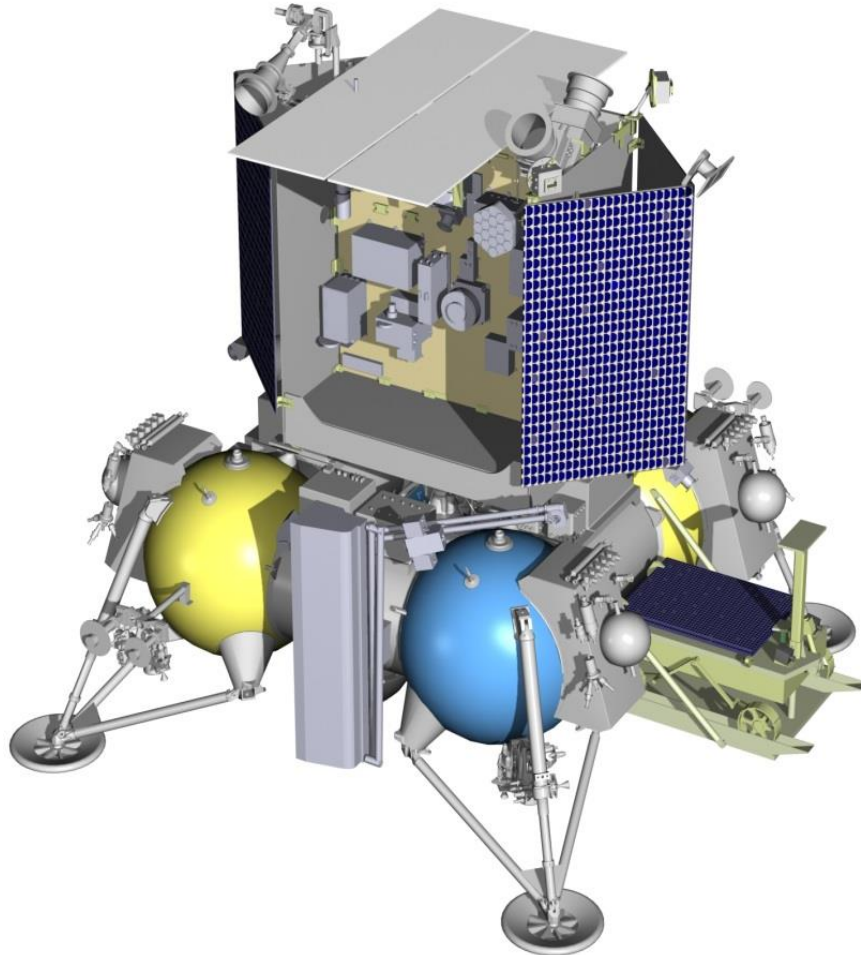
Common logarithm of the dust density in particle per cubic meter at the local lunar evening (top) and sunset (bottom). The sun is on the right,  $11^\circ$  (top) and  $1^\circ$  (bottom) above the horizon. IS from the PmL instrument location marked by "X" sign.





# Luna-27 (Luna-Resource Lander)

## Expected results



## Technology:

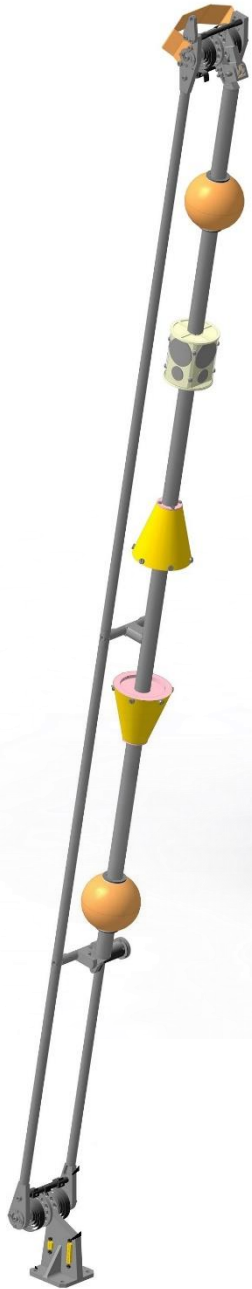
- High precision landing and hazard avoidance
- Pole-orbiter UHF radio link tests and experience
- Cryogenic drill testing and validation

## Science:

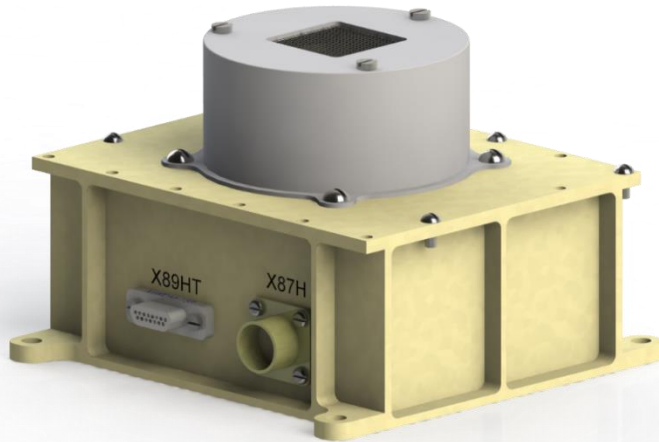
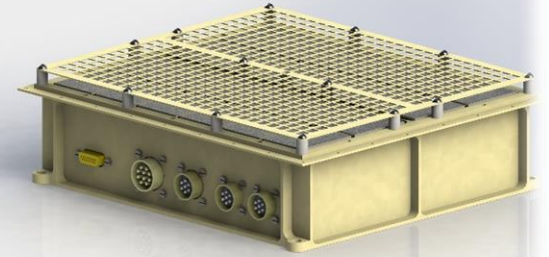
- Mechanical/thermal/compositional properties of polar regolith within 2 meters
- Water content and elements abundance in the shallow subsurface of the polar regolith
- **Plasma, neutral and dust exosphere at the pole**
- Seismometry and high accuracy ranging

# PmL-LR Instrument

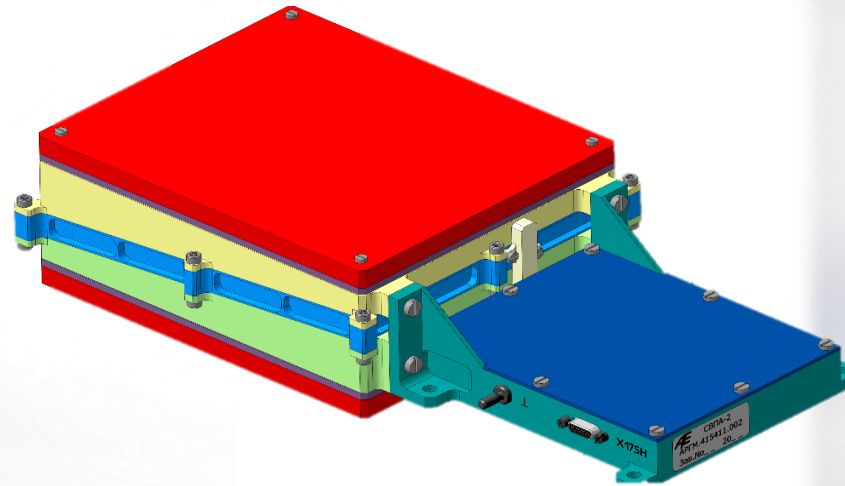
Boom (2xLPs, 2xEPs, IS)



2x  
Impact Sensor



SWDA-1



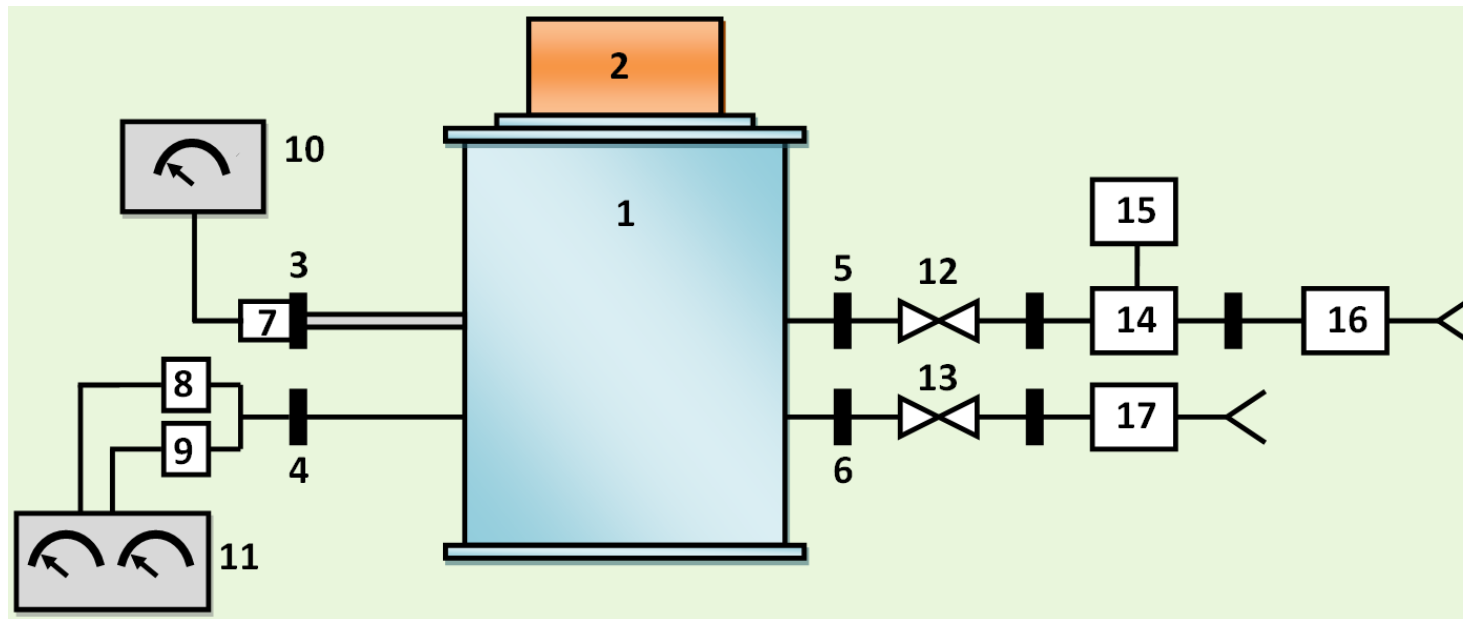
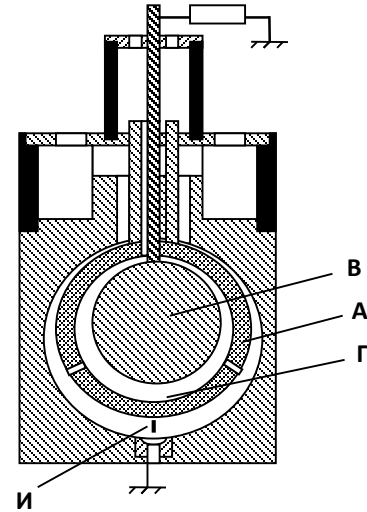
SWDA-2



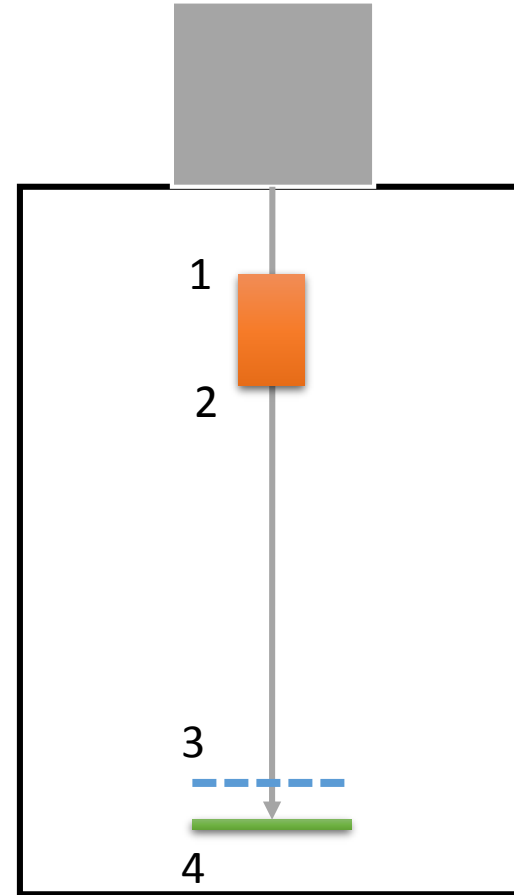
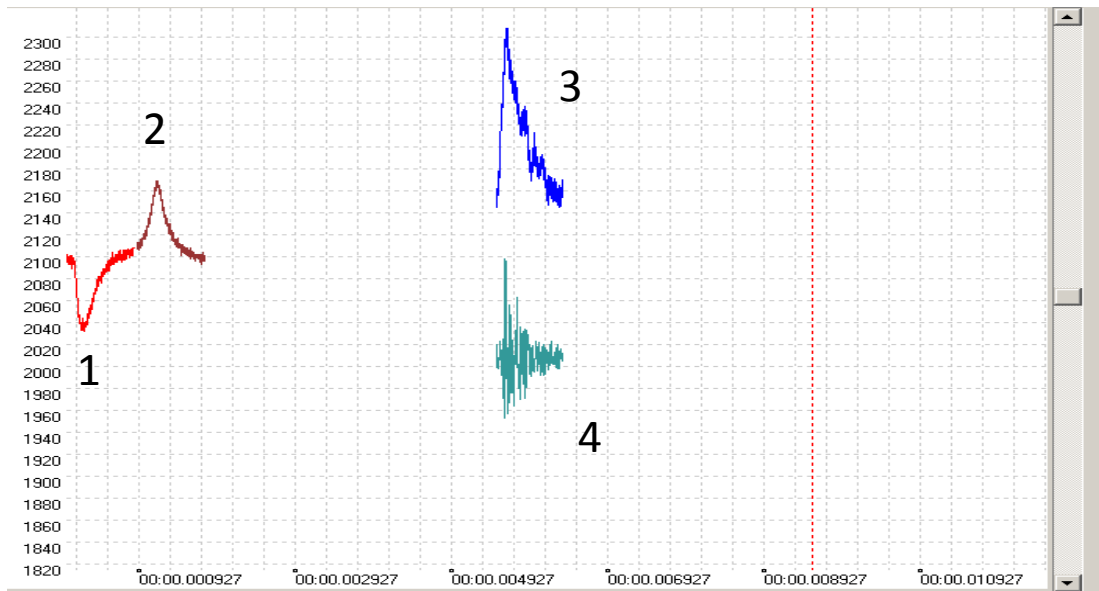
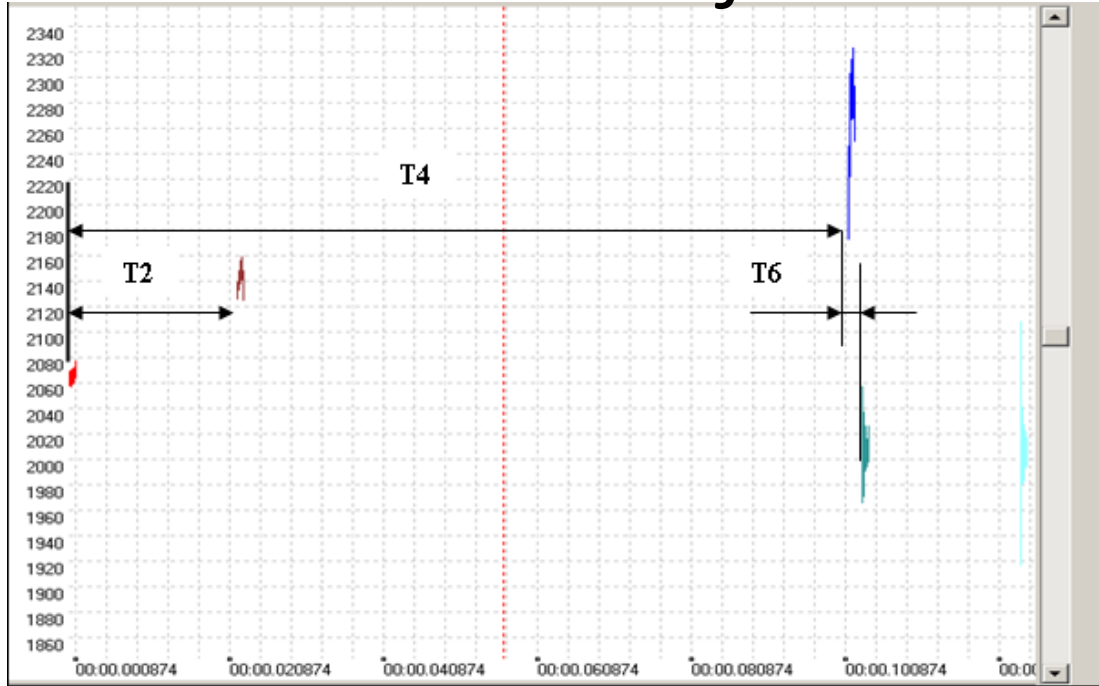
2xEP

# The Experimental Set-up for the Lunar Dust Particles Investigation and Instruments calibrations

- Pressure  $< 1,01325$  Pa
- Injected particles:
  - particle size  $1 \div 300 \mu\text{m}$
  - velocity  $10 \div 100$  m/s
  - charge  $\geq 1000e^-$



# Injected microparticles



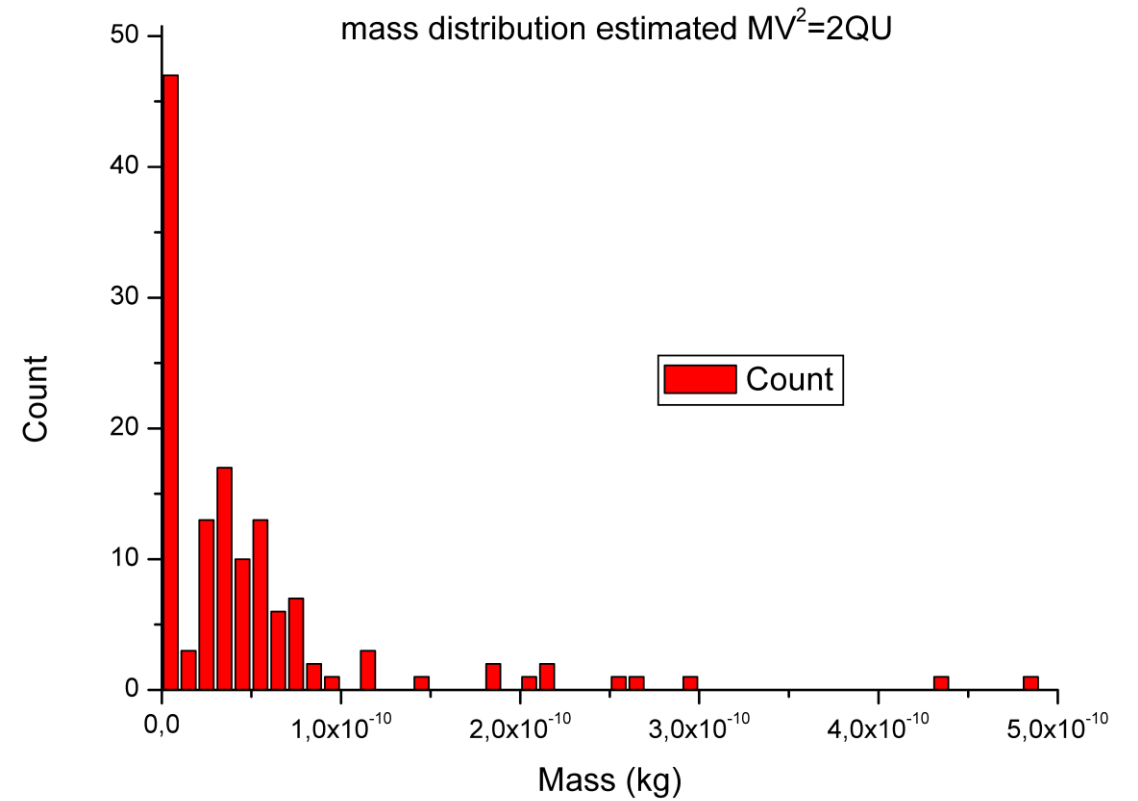
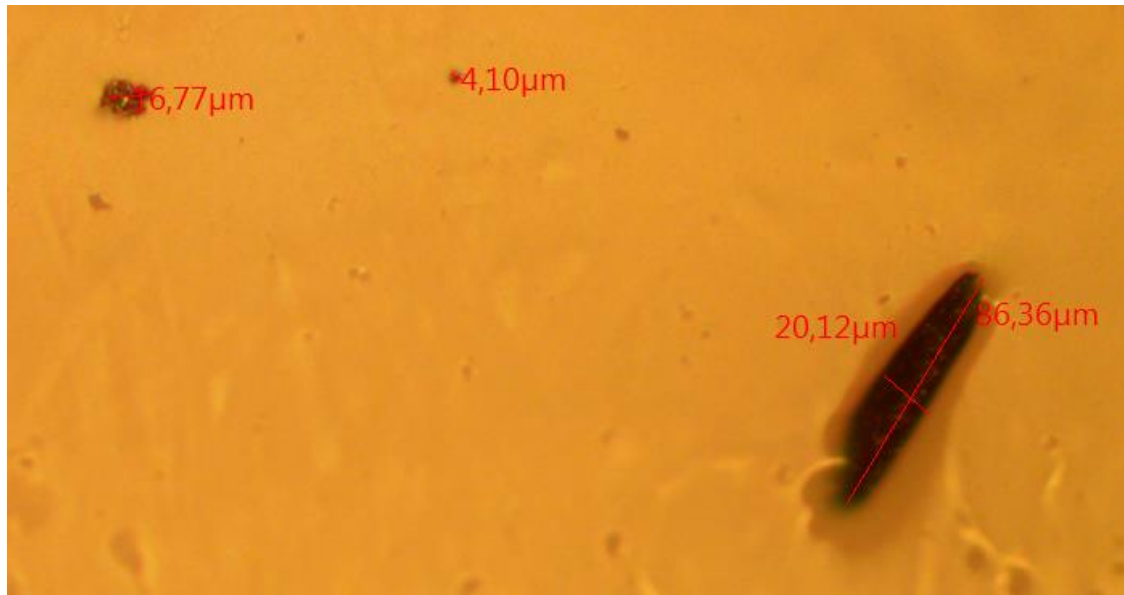
Dust Injector

Inductive Sensor

Charge-sensitive inductive grid

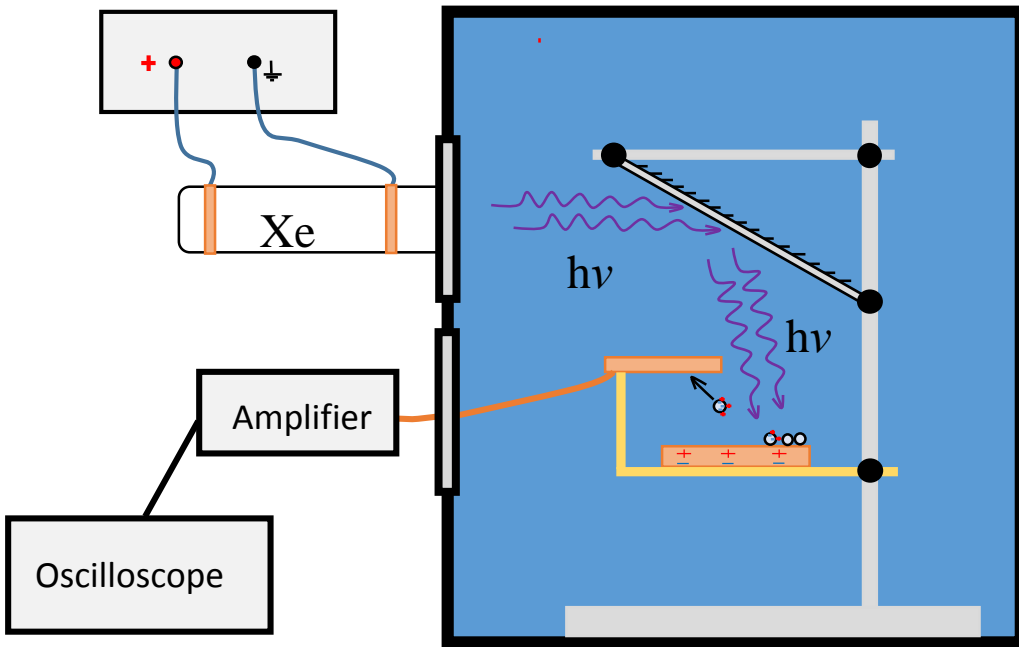
Momentum PZT sensor

# Injected microparticles



W (20-40  $\mu\text{m}$ )

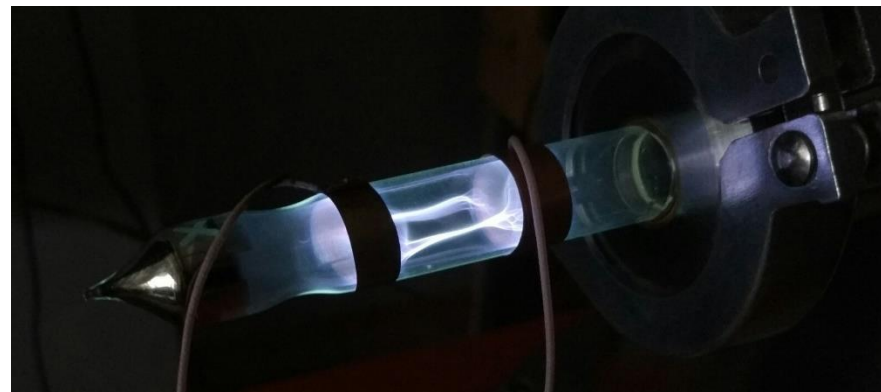
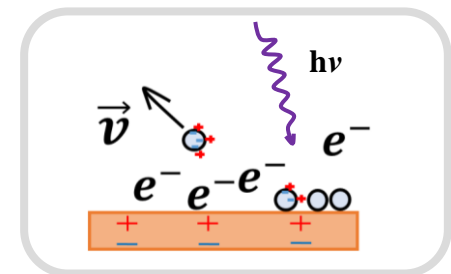
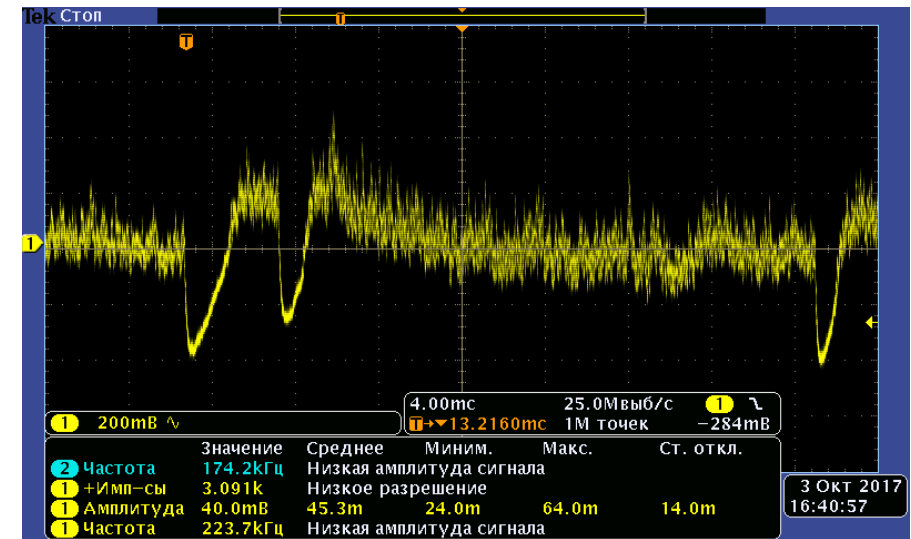
# UV Source



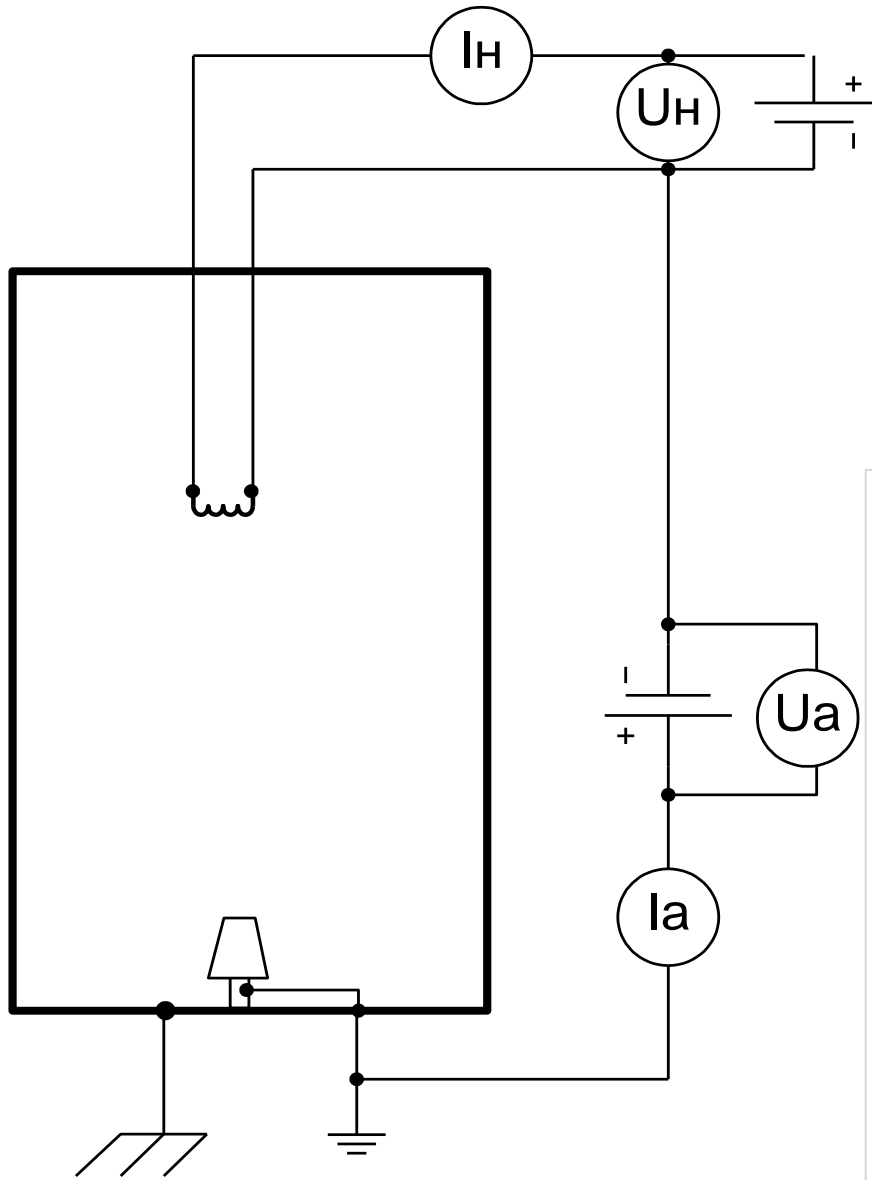
UV source here is Xe excimer lamp (172 nm).

The material is 20  $\mu\text{m}$  dielectric glass spheres.

As a result we can see a lot of events, which only can be connected with electrostatically lift-off of charged by UV particles.

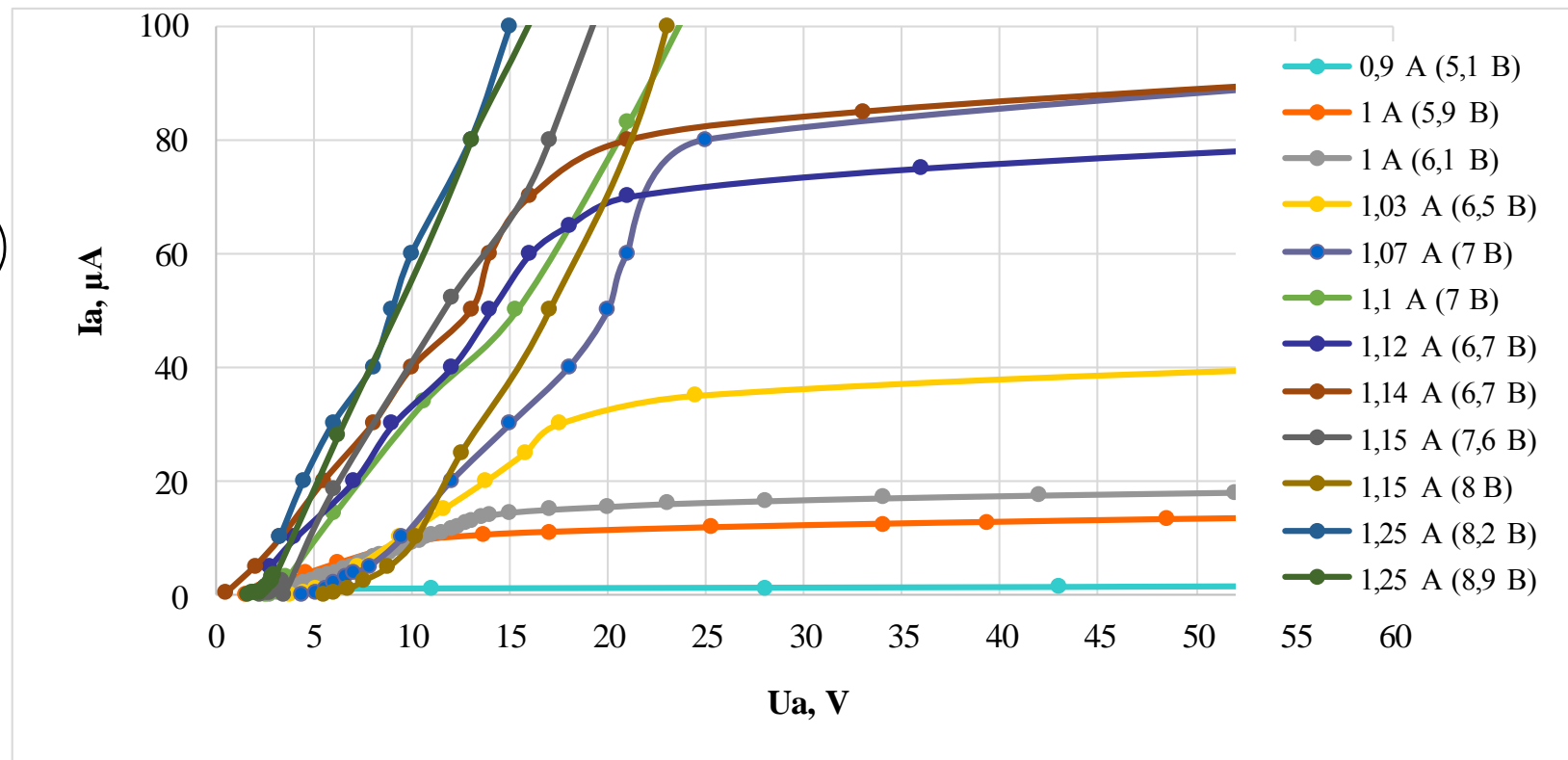


# e Source



- Electron source: W
- $T_e = 4,3..50$  eV
- Pressure:  $10^{-3}$  torr
- $T_w = 2800..3300$  K

$$T = \frac{R - R_0}{\alpha \cdot R_0} + T_0$$



# Further investigation

- The next step is to simulate detailed parts of SC, especially Langmuir probes and its interactions during the measurement time.
- Critically important to simulate SC-plasma interactions in the case of developing Luna-27 (Luna-Resource) - especially dust instrument units.
- Simulation of dusty plasma conditions inside the set-up vacuum chamber with various irradiation and particle sources.
- Simulation of Instrument(SC)-plasma interactions for various solar system atmosphereless bodies.



# Summary and conclusions

- We can see that the SPIS-DUST code seems to be a powerful tool for the simulation of the Lander electric charging and the Lander plasma-dust environment interactions and can be very useful both for instrument development and for lander's data analysis.
- The SPIS-Dust tool has been applied to a variety of cases and is a solution for estimating dust contamination risks and for designing mitigation techniques, as a complement to ground testing. The genericity of the model will enable to add physical modules (as e.g. micrometeorite impact, large scale simulations) and upgrade detailed models for dust interactions in the case of future Russian Luna-Glob and Luna-Resource Landers.

# Thank you!

I.A. Kuznetsov et al., *Numerical Modelling of Plasma-Lunar Lander Interactions*, Planetary and Space Science 156 (2018) 62–70, <https://doi.org/10.1016/j.pss.2018.03.004>

This work was supported by the Russian Scientific Foundation (the grant № 17-12-01458).